Investigation on Cirrus Clouds Ice Nuclei Characteristics and their effect on Optical Properties

Reji K Dhaman[1], Malladi Satyanarayana[2]

[1](Department of Optoelectronics, University of Kerala, Karyavattom, Trivandrum, India)
[2](Department of ECE, VNR Vignana Jyothi Institute of Engineering & Technology, Hyderabad, India)

Abstract:
Background*: The cirrus ice nuclei characteristics and its effect on the optical properties were investigated from the National Atmospheric Research Laboratory (NARL; 13.5^0N, 79.2^0E), Gadanki, Andhra Pradesh, India, an inland tropical station during the period of observation January 2009 to December 2010. From the observations the cirrus ice nuclei characteristics such as effective radius (R_e), ice water content (IWC), ice water path (IWP), ice nuclei concentration (INC), ice crystal fall velocity (V_m) were studied. The variation of these tropical ice nuclei properties with mid cloud temperature were also studied. The present study may be useful in predicting the effect of ice nuclei on the cloud dynamics, precipitation and climatology.*

Materials and Methods*: The ground based lidar system installed at Gadanki was operated during clear sky conditions and free from low level clouds. Typically, about 4–6 hours of observations were made during each observation day at night from 22:00 to 05:00 Indian Standard Time (IST; corresponding to 82.5°E). Also, it was aligned to an overlap altitude of greater than 4km in order to avoid the intense backscattered signals from the low altitude clouds and aerosols. For the present analysis, all the temperature observations were taken from radiosonde experiments conducted at the station during the same period. MST Radar observations were taken for the vertical wind transport analysis. The complex time series of the decoded and integrated signal samples are subjected to the process of FFT for on-line computation of the Doppler power spectra for each range. The data processing for parameterization of the Doppler spectrum involves the removal of dc, estimation of average noise level, incoherent integration and computation of the three low order moments.*

Results*: The cloud mean IWC ranged from $2.08x10^{-5}$ to $1.22x10^{-3}$ g/m^3 for the period 2009 and from $3x10^{-5}$ to $6x10^{-3}$ g/m^3 for 2010. The IWP for the SVC was low (<0.2 g/m^2), for TC, IWP lie in the range $0.2<IWP<4$ g/m^2 and for DC, $IWP>4$ g/m^2. The IWC was strongly dependent with the INC and effective size of the ice particle. Observed cirrus with slow updrafts were very thin with low IWC and INC; cirrus with fast updrafts were thick with high IWC and INC.*

Conclusion*: The effective radius of ice crystal was dependent on the ambient temperature and it showed a maximum at the cloud bottom and minimum in the cloud top. Ice crystals formed on the cloud top layer were small in size and less ordered. The ice nuclei concentration and ice water content showed strong correlation. The higher ice water content was most frequently observed at the lower altitude where the temperature was warm and the ice crystals formed were aggregates. Cirrus formed by slow updrafts were thin with low ice water content and ice nuclei concentration while cirrus with fast updrafts were thick with high ice water content and ice nuclei concentration.*

Key Word*: Lidar; Radar; Ice nuclei; Fall velocity; Cirrus.*

I. Introduction

Cirrus clouds are widely distributed in the upper troposphere and lower stratosphere (UTLS) region and they cover about 30% of the total Earth's surface[1]. Cirrus clouds have significant effects on Earth's radiation budget in regulating two important radiative effects, namely, greenhouse effect and albedo effect[2, 3]. These radiative effects are strongly depending on the cirrus macrophysical and microphysical properties of the ice crystals present over there. Characterizing the above properties of the cirrus clouds will enhance the understanding of the formation of cirrus, their influence and dynamics on the radiation budget. The mechanism for the formation of ice particles in the atmosphere, remain poorly understood[4]. The interactions of radiation with ice clouds are mentioned by the single-scattering properties of ice clouds such as ice water content (IWC), ice water path (IWP) and the effective size of the cloud particles[5]. The ice crystal shape in cirrus varies with change in cloud temperature. The cirrus cloud particles are generally polycrystalline in shape at temperatures ranging from -20°C to -40°C[6,7], while at temperature below -50°C they are single crystals, predominantly hollow or solid columns. Observations of Heymsfield and Miloshevich [1995] showed a fast transition from

---

water droplet to ice crystal characteristic of homogeneous ice nucleation in the temperature range -35°C to -56°C[8]. The cloud mean altitude and mid-cloud temperature play an important role in determining cloud radiative properties. As a result, it is necessary to understand the ice cloud parameters which have a significant role in cloud formation and dynamics. In view of this, an attempt to systematic study of ice cloud parameters is done and their variation with mid-cloud temperature, altitude and extinction are studied.

II. Material and Methods

The instruments used for the determination of cirrus cloud microphysical and optical properties have already been well explained by Dhaman et al.[2016][9]. The ground based lidar system at Gadanki was operated during clear sky conditions and free from low level clouds. Typically, about 4–6 hours of observations were made during each observation day at night from 22:00 to 05:00 Indian Standard Time (IST; corresponding to 82.5°E). There are either less or no observations during the monsoon period mainly due to limitations of optical system availability for operating during clear sky conditions. Also, it was aligned to an overlap altitude of greater than 4km in order to avoid the intense backscattered signals from the low altitude clouds and aerosols. Observations are carried out during the period from January 2009 to December 2010. The cirrus cloud data observed during the 32 days out of the 43 days of observation are used for the cirrus ice nuclei characteristics and its radiative properties. For the present analysis, all the temperature observations were taken from radiosonde experiments conducted at the station during the same period. The MST radar at the station is a monostatic coherent pulse Doppler radar operating at 53 MHz with a peak-power aperture product of 3×10^{10} Wm^2 [Rao et al.1995]. The antenna system occupying an area of 130 m×130 m is a phased array of 32×32 three-element Yagi antennas consisting of two orthogonal sets, one for each polarization (magnetic E–W and N–S)[10]. It generates a radiation pattern with the main lobe of 3° width (between 3 dB points), gain of 36 dB and first side lobe level of −20 dB. The main beam can be positioned at any look angle within ±20° off zenith in the two major planes (E–W and N–S). The numbers of FFT points are up to 512 and coherent integrations are from 4 to 512 (selectable in binary steps). The pulse widths can be encoded from 1 to 32 μs (in binary steps) and can be coded from 16 to 32 μs with 1 μs band length.

Procedure methodology

For estimating the average noise level in MST Radar, an objective method developed by Hildebrand et al. [1974] has been adopted here[11]. Optical properties of cirrus, which are vital for the cloud radiative effects, can be derived from LIDAR observations. The cloud extinction coefficient is obtained by the widely used [Klett, 1981] LIDAR inversion methods[12]. A range independent LIDAR ratio (LR) is used in these techniques for retrieving the extinction coefficients. Making use of the LIDAR system constants and from the measured backscattered signal power, the extinction coefficient of the clouds is determined by inverting the LIDAR signals as described by Klett.

The optical depth (τ_c) of the cirrus cloud can be obtained from LIDAR data using the equation,

$$\tau_c = \int_{h_{base}}^{h_{top}} \alpha(h)dh$$

where $\alpha(h)$ is the extinction coefficient within the cloud region, which extends from cloud base (h_{base}) to cloud top (h_{top}). Based on optical depth, cirrus clouds are classified into sub-visual cirrus (SVC) ($\tau_c < 0.03$), optically thin cirrus (TC) ($0.03 < \tau_c < 0.3$) and dense cirrus (DC) or opaque clouds ($0.3 < \tau_c < 3.0$)[13].

Parameterization of Cirrus Ice Nuclei Properties

1. Ice Nuclei Effective Radius

Ice nuclei effective radius, r_{eff}, is parameterized as a function of temperature[14], following (Ivanova et al, 2001):

$$r_{eff} = (75.3 + 0.5895 * T)/2 \text{ (in microns)},$$

where T is in ^{0}C. The effective radius is a measure of the particle size used to calculate the optical properties of clouds along with it provides additional information for the ice cloud radiative characteristics. The values of r_{eff} are in sharp contrast with many parameterizations currently in use in climate models. It represents r_{eff} as a function of both temperature and ice water content[15].

2. Ice Water Content

Cloud ice water content (IWC) is defined as cloud ice mass in unit volume of atmospheric air. It can vary largely from 0.0001 g/m^{3} in thin cirrus to 1 g/m^{3} inside convective core. The ice water content (IWC) of

cirrus clouds is of particular interest because it is measurable and it can be directly related to radiatively important variables such as extinction and effective radius. One of the most common ways to parameterize ice cloud properties in models is to use IWC[6]. The cirrus extinction coefficient as well as the IWC depends upon the particle size distribution (PSD) of an ice particle ensemble, which provide the determination of IWC from extinction measurements. Thus, IWC and extinction are approximately proportional to each other. The IWC is calculated by using the equation,

$$IWC = \frac{2}{3} \rho_{ice} r_{eff} \alpha(h),$$

where ρ_{ice} = 920 g/m^3(density of solid ice), r_{eff} = ice nuclei effective radius and $\alpha(h)$ = cirrus extinction coefficient.

3. Ice Water Path

The cirrus ice water path (IWP) is defined as the integral of the ice water content (IWC) along the depth of an ice cloud layer. It has a significant importance in climate studies as it is critical for determining cloud absorption, optical depth[16, 17], and emissivity. IWP is determined by using the equation,

$$IWP = \int_{h_{base}}^{h_{top}} IWC(h) \, dh$$

4. Ice Nuclei Concentration

Ice crystals within cirrus clouds are formed in a variety of mechanisms. Heterogeneous nucleation mechanism refers to the formation of ice on an aerosol surface, and the portion of aerosol upon which ice forms this way are called ice-nucleating particles (INP). Ice crystals may also form via homogeneous nucleation, typically at temperatures below about 235 K[18]. For the determination of Ice Nuclei Concentration (INC), we have adopted a power law that has been widely used to represent the relation between INC and effective radius, and is given by the equation,

$$INC = \frac{4}{3\pi r_{eff}^2} \alpha(h),$$

where r_{eff} = ice nuclei effective radius and $\alpha(h)$ = cirrus extinction coefficient.

5. Ice Crystal Fall Velocity

Sedimentation (fall-out) of ice crystal is an important process that occurs in clouds and has a large influence on their microphysical as well as radiative properties. In situ measurements[19] have shown that cirrus clouds top is mainly composed of small but abundant ice crystals, whereas the bottom consists more of few large crystals. Such vertical distributions cause local cooling or warming radiative effects[20]. The ice crystal fall velocity (V_m) is estimated following Mitchell et al., [2011] as

$$V_m = 0.0205 * D_{eff}^{1.69}, \qquad D_{eff} \leq 51\mu m$$
$$V_m = 0.805 * D_{eff} - 25.4, \quad D_{eff} > 51 \ \mu m$$

where D_{eff} is the effective diameter of the ice crystal.

III. Results and Discussion

The cirrus cloud data observed during the 32 days out of the 43 days of observation were used for the cirrus ice nuclei characteristics and its radiative properties. For the present analysis, all the temperature data were taken from radiosonde experiments conducted at the station during the same period. Figure 1 shows the vertical profile of the ice nuclei properties observed on one of the cirrus occurrence day. From the figure it can be seen that ice crystal size generally increases downward in a cirrus cloud layer. Also, the ice sedimentation velocity will increase with decrease in altitude. The cirrus extinction coefficient and IWC showed the similar trend of decrease in magnitude as altitude increases. In the cloud region, both started increasing reached a maximum at the mid-cloud and decrease at the cloud top. The INC will be maximum at the mid-cloud region than cloud base and top. The detailed investigation and its effect on radiative properties are explained in the following sections.
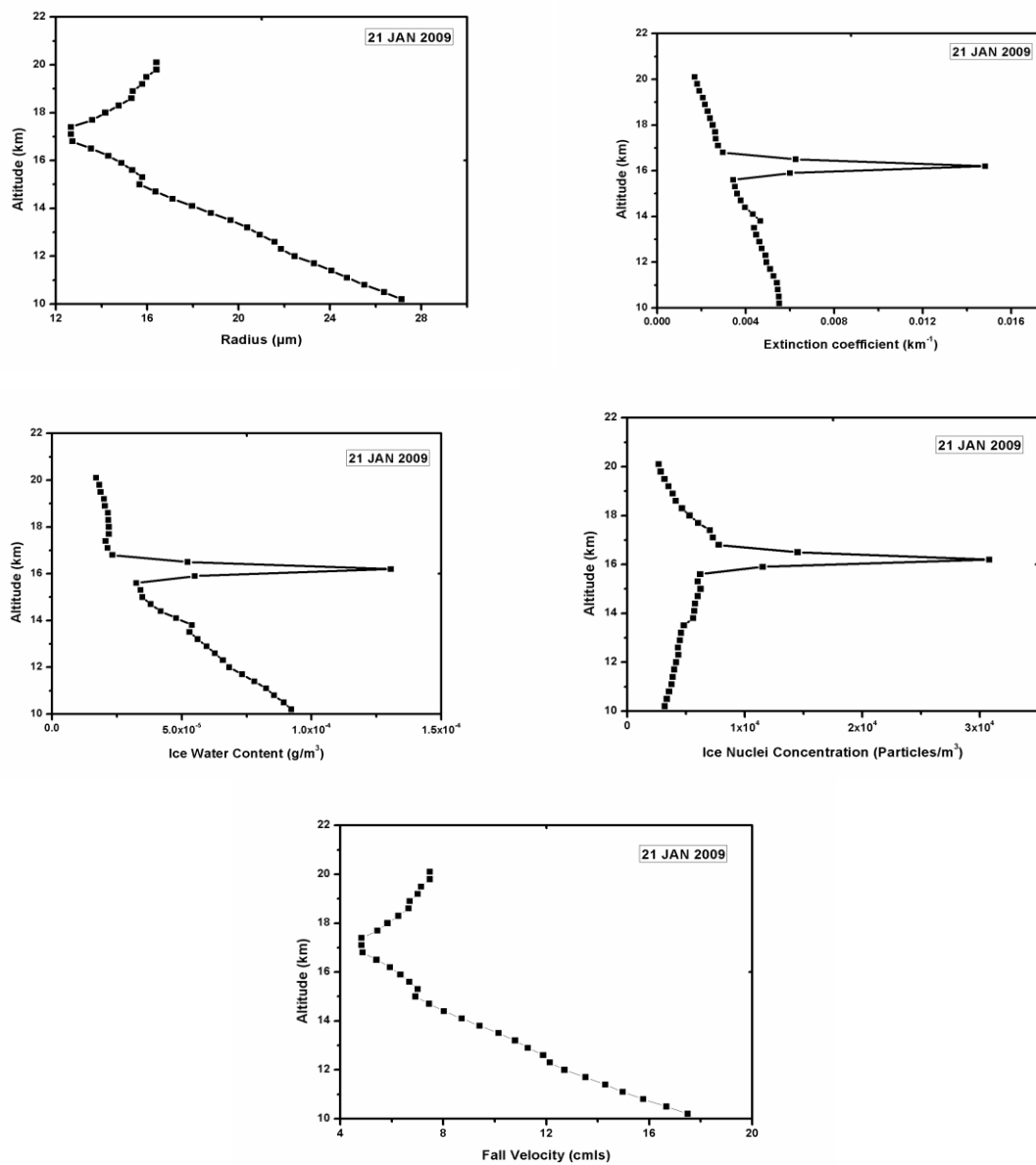
Figure 1: Vertical profiles of cirrus ice nuclei properties (a) Effective radius (b) Extinction coefficient (c) Ice water content (d) Ice nuclei concentration and (e) Fall velocity.

Ice Nuclei Effective Radius

Ice nuclei effective radius, r_{eff} is a measure of the average size of the particles comprising in a cloud region. Since the ice crystal size is dependent on the ambient temperature it showed maximum at the cloud bottom and minimum in the cloud top. From figure 1 it was clear that the cirrus extinction at the top altitudes were low and the ice crystal size were relatively small. This shows that most of the cirrus clouds observed at higher altitudes were thin. Above the cloud top altitude cirrus extinction coefficient decreases but the size of the particles increases and this is due to the heterogeneous formation by the activities in the lower stratosphere. Figure 2 presents the cloud mean variation of r_{eff} during the cirrus occurrence days for the year 2009 and 2010.
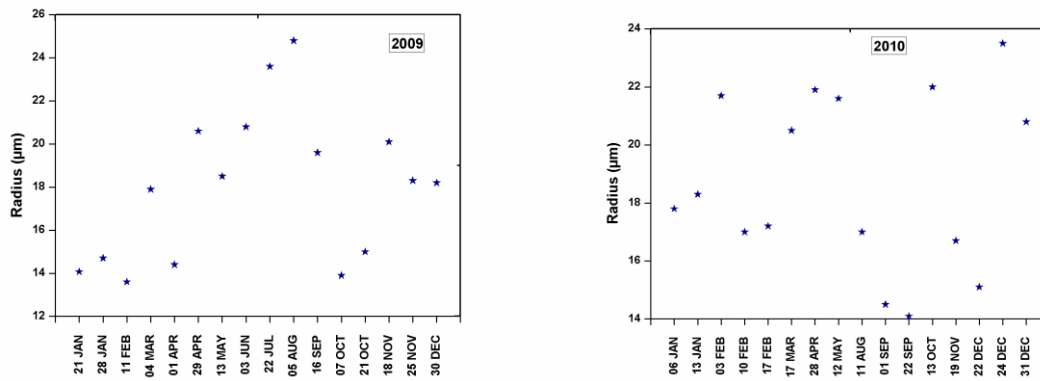
Figure 2: Cloud mean variation of cirrus ice nuclei effective radius during the cirrus occurrence days.

From figure 2, it is clear that the observed cirrus mean effective radius showed a maximum of 24-25 µm and the sizes were generally maximum in the monsoon period. The cirrus clouds formed over the tropics were mainly due to the prevailing convective activities, which transport the water vapor and the aerosol particles present over there to the upper troposphere. Hence the size of the ice crystals will enhance and show higher depolarization ratio.

Figure 3 represents the plot of monthly mean cirrus ice nuclei radius with cirrus mid-cloud temperature and cloud mean altitude during the observation period. It can be seen that the ice crystal size decreases, with increase in altitude and decrease in temperature.
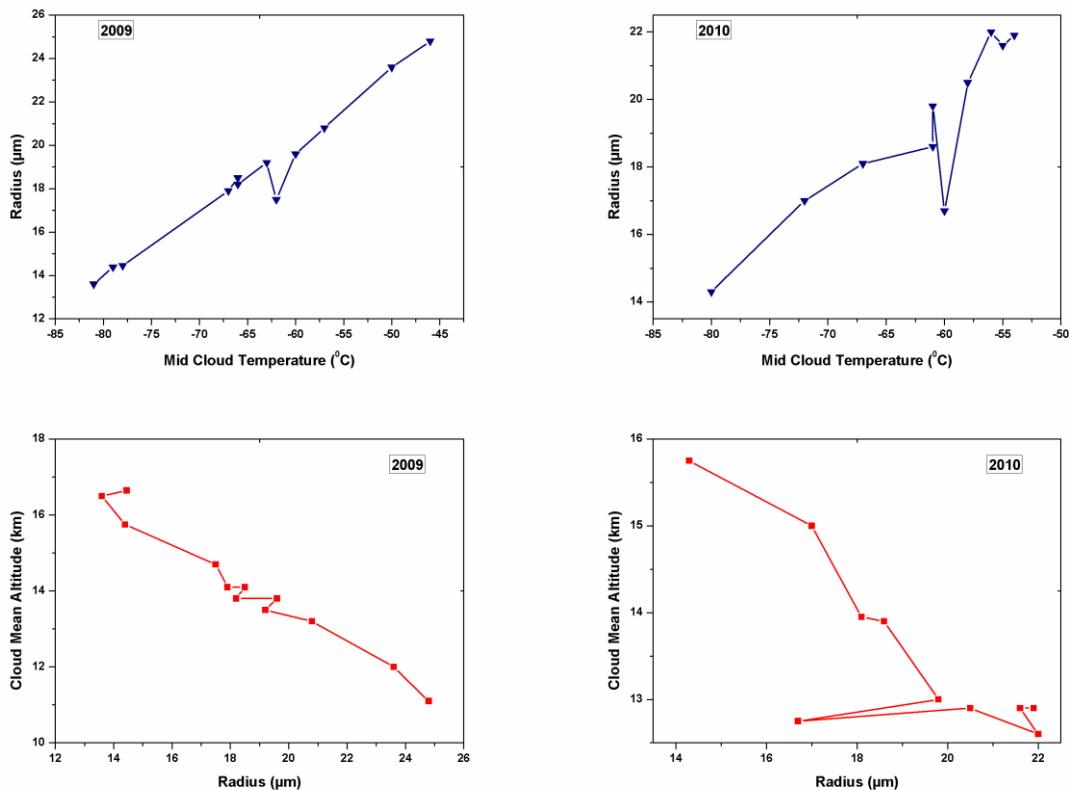

Figure 3: Monthly mean cirrus ice nuclei effective radius with (a) cirrus mid-cloud temperature and (b) cloud mean altitude.

Ice Water Content

Ice water content (IWC) is one of the microphysical properties of cirrus that is essential for better describing the radiative effect[22]. IWC is related to particle size and extinction, both of which are used for determining the radiative properties of cirrus cloud. From figure 1, it is evident that cirrus IWC showed a

maximum at the mid-cloud region compared to cloud base and top. Figure 4 presents the mean cloud IWC during the cirrus occurrence days for the year 2009 and 2010. It was observed that during 2010 IWC was higher than for the period 2009. Also, for the period of observation 2009 (2010) IWC showed the peak in the month of August (December). This period indicates the occurrence of dense cirrus. The cloud extinction was also high in this region. Also, it is noticeable that for the period 2009 (2010), almost 87.5% the IWC lie in the range 2×10^{-4} g/m^3 (1×10^{-3} g/m^3). During the period of monsoon IWC increased. The cloud mean IWC range from 2.08×10^{-5} to 1.22×10^{-3} g/m^3 for the period 2009 and from 3×10^{-5} to 6×10^{-3} g/m^3 for 2010.
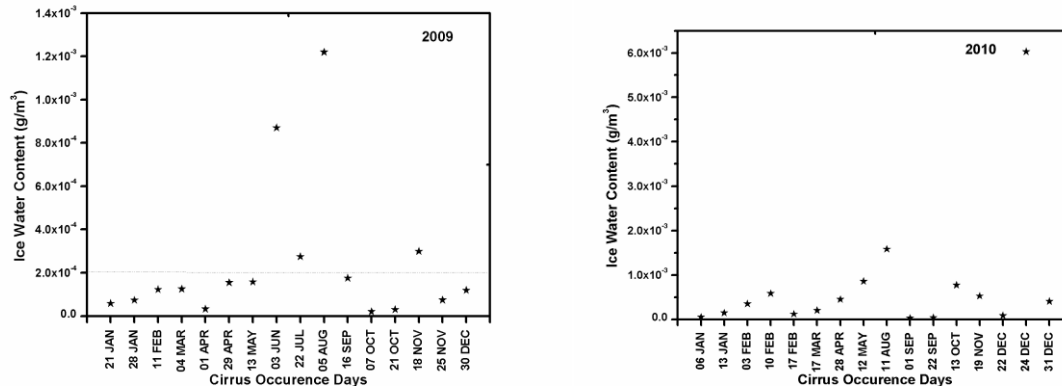

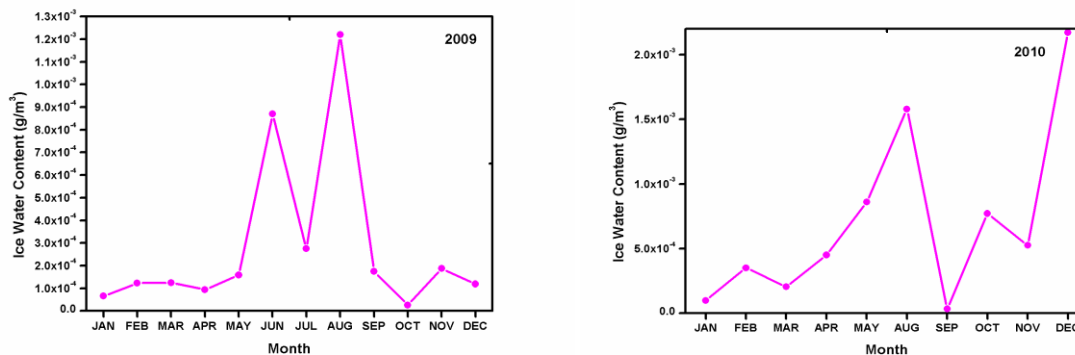**Figure 4:** Cloud mean IWC during the cirrus occurrence days for the period 2009 and 2010.

Figure 5: Monthly mean cirrus IWC during the period of observation 2009 and 2010.

Figure 5 presents the monthly mean cirrus IWC for the period 2009 and 2010. It can be seen that the IWC was maximum in the monsoon period, where the relative humidity (RH) in general will be high. The relative humidity in the atmosphere is a key factor for the ice initiation. For the formation of ice in a clear sky, the RH should attain a particular threshold by the dynamic process such as vertical updraft motion. Once the ice particles are formed, they start growing by the consumption of surrounding water vapor. The magnitude of IWC will vary for different types of cirrus clouds and that depends on the altitude, temperature and RH[23]. Figure 6 presents the variation of IWC with mid-cloud temperature during the period of observation. For the period 2009, it was observed that the IWC decreases with decrease in mid-cloud temperature. But for the period 2010, even though the trend was decrease in nature, at certain temperature regions IWC showed a peak which signifies the presence of large cloud condensation nuclei (CCN) present over there. Also, it was clear that the lower temperature region had low IWC and the higher temperature of high IWC, which indicates that the low IWC correspond to heterogeneous ice nucleation and high IWC led to the homogeneous ice nucleation. The higher IWC are most frequently observed at the lower altitudes where the temperature is warm and the ice crystals formed are considered as aggregates[24].
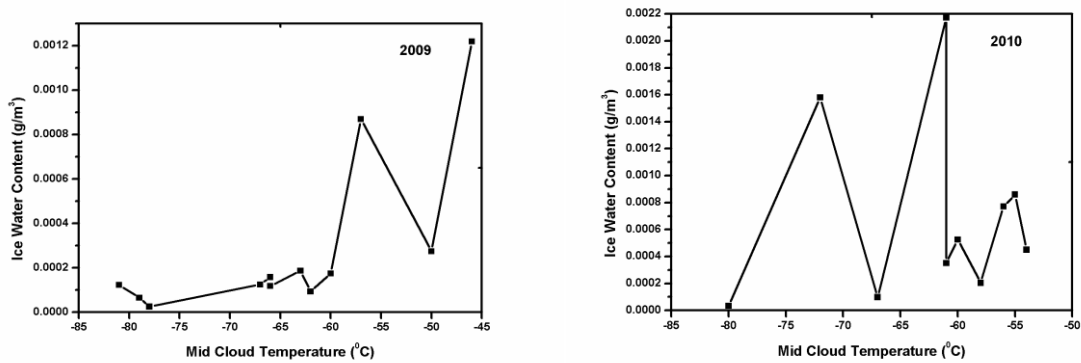
Figure 6: Variation of cirrus IWC with mid-cloud temperature during the period of observation 2009 and 2010.

Ice Water Path

The cirrus ice water path (IWP) is defined as the integral of the ice water content (IWC) along the depth of an ice cloud layer. Figure 7 presents the monthly variation of IWP during the period of observation. IWP showed a maximum over the monsoon period and the variability of IWP depends on the cloud composition and the presence of IWC. During the monsoon season there was a large transport of aerosols and water vapor to the high altitudes by convection. This enhanced the ice nuclei concentration and the IWC within the cloud which made IWP to be high. Also, it was observed that IWP had a strong correlation with optical depth of cirrus clouds. Based on optical depth, cirrus clouds are classified into sub-visual cirrus (SVC) (τ_c<0.03), optically thin cirrus (TC) (0.03<τ_c< 0.3) and dense cirrus (DC) or opaque clouds (0.3<τ_c< 3.0). It was observed that for the SVC the IWP was low (IWP<0.2 g/m^2), for TC, IWP lie in the range 0.2<IWP<4 g/m^2 and for DC, IWP>4 g/m^2.
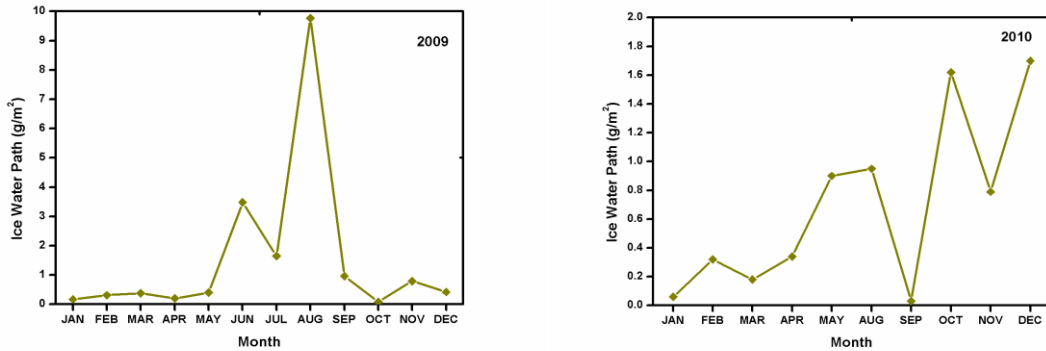

Figure 7: Monthly mean cirrus IWP for the period 2009 and 2010.

The variation of IWP with cirrus mid-cloud temperature was also studied. Figure 8 presents the variation of IWP with mid-cloud temperature. IWP showed a strong positive correlation with mid-cloud temperature for both observation periods.
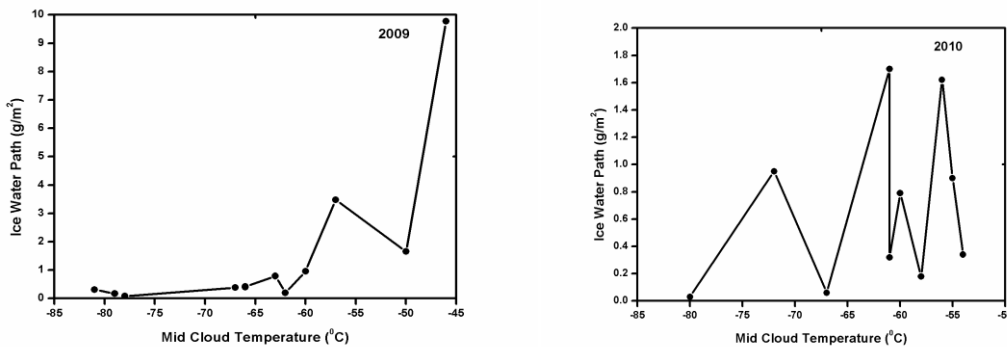

Figure 8: Variation of cirrus IWP with mid-cloud temperature during the period of observation 2009 and 2010.

Ice Nuclei Concentration

Ice crystals within cirrus clouds were formed in a variety of mechanisms. Heterogeneous nucleation mechanism refers to the formation of ice on an aerosol surface, and the portion of aerosol upon which ice forms this way are called ice-nucleating particles (INP). Ice crystals may also form via homogeneous nucleation, typically at temperatures below about 235 K[25]. Figure 9 presents the monthly variation of INC during the period of observation. For the period 2009, the mean INC range from $5.7x10^3$ to $6.7x10^4$ particles/m^3 with a standard deviation of $2x10^4$ particles/m^3. INC showed a maximum in the monsoon period. For the period 2010, INC range from $7.4x10^3$ to $2.2x10^5$ particles/m^3 with a standard deviation of $6.5x10^4$ particles/m^3. For the period 2010 also, the INC showed maximum in the monsoon period. During the monsoon season due to large convective activities there is a large transport of aerosols and water vapor to the high altitudes. This enhances the ice nuclei concentration and the IWC within the cloud. Also, it was observed that whenever large INC occur the size of the ice nuclei was less. The variation of INC may range up to several orders of magnitude when the sizes of the ice nuclei were small.
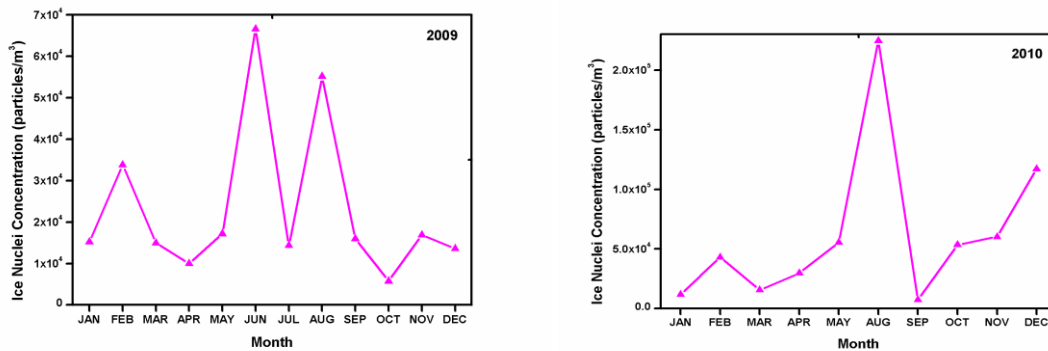

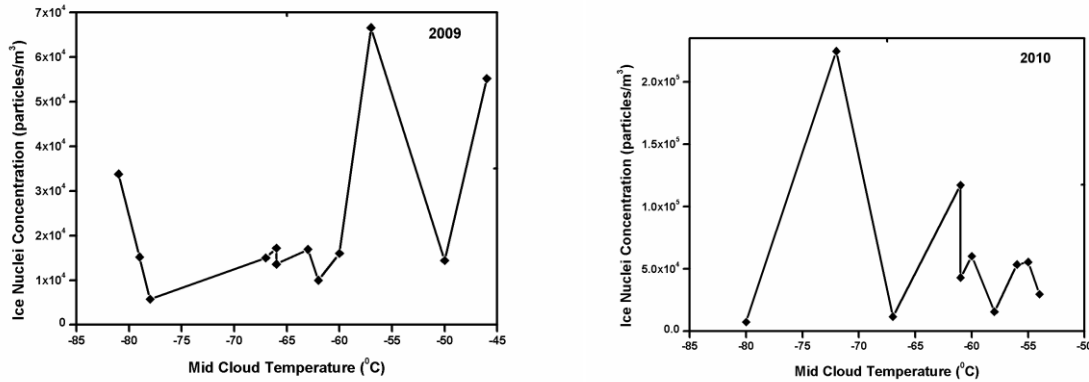**Figure 9:** Monthly mean cirrus INC for the period 2009 and 2010.

Figure 10: Variation of cirrus INC with mid-cloud temperature during the period of observation.

Figure 10 shows the variation of INC with mid-cloud temperature during the observation period. From the figure it was clear that as the temperature decreases, the ice particle concentration was either constant or increases slightly. High ice concentrations are observed sometimes during the strong updrafts that results from homogeneous nucleation. The observed results are in agreement with Lawson et al., [2008] and Krämer et al., [2009] who reported the INC are typically 100 particles/liter[26, 27]. The IWC was strongly dependent with the INC and effective size of the ice particle. For better understanding of the relationship between INC an IWC, a correlation study was taken with these parameters. Figure 11 presents the values of IWC versus INC.
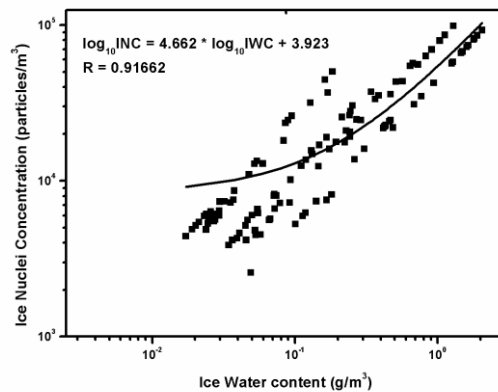
Figure 11: Values of cirrus ice water content (IWC) versus ice nuclei concentration (INC).

It was observed from the figure that INC increases with increasing IWC, even though the INC varies widely. The linear fitting (in the log − log coordinate) was shown with a thick dash line. The linear fitting equation is given by, $\log_{10}\text{INC} = 4.662 * \log_{10}\text{IWC} + 3.923$

The correlation coefficient R (=0.91) indicates that INC is significantly correlated to the IWC. INC and IWC are in the units of particles/m^3 and g/m^3 respectively.

Ice Crystal Fall Velocity

The fall velocity is the rate at which an ice crystal falls through a cloud and depends on the ice crystal mass, size and shape. The sedimentation (fall-out) of ice crystal is an important process that occurs in clouds and has a large influence on their microphysical as well as radiative properties. In situ measurements have shown that cirrus clouds top is mainly composed of small but abundant ice crystals, whereas the bottom consists more of few large crystals[19]. Such vertical distributions cause local cooling or warming radiative effects. Figure 12 presents the cloud mean variation of fall velocity of ice crystals present during the cirrus occurrence days for the year 2009 and 2010.
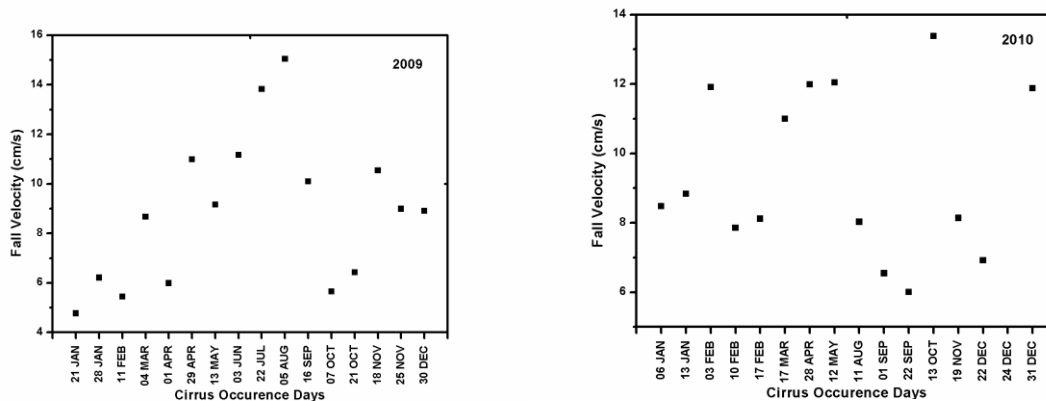

Figure 12: Cloud mean ice fall velocity during the cirrus occurrence days for the period 2009 and 2010.
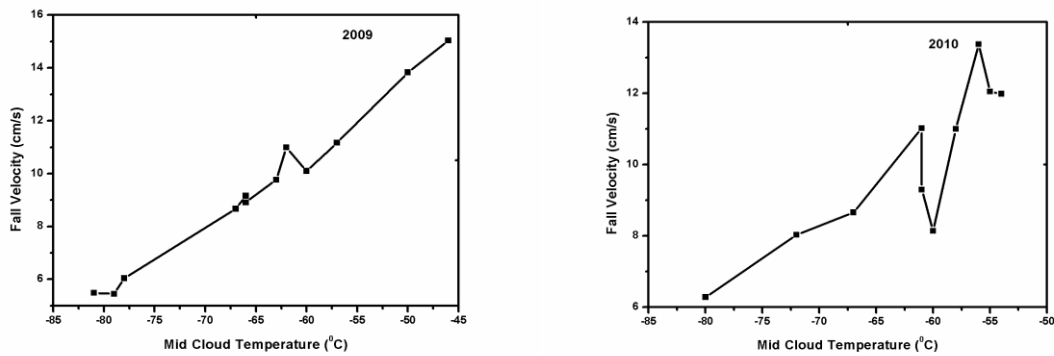
Figure 13: Variation of cirrus ice crystal fall velocity with mid-cloud temperature during the period of observation.

Figure 13 presents the variation of ice crystal fall velocity with mid-cloud temperature during the period of observation. It was clear that fall velocity increases with increase of temperature, consistent with the general behaviour of the tropical cirrus clouds. This showed that the size of the ice crystals formed was comparatively shorter at higher altitude with lower temperature and falls out slowly. The lower temperature region enhances the homogeneous ice nucleation mechanism[28]. From figure 3(a) and 13, it was obvious that the fall velocity varied linearly with effective size of the ice crystals. The results obtained were in agreement with *Heymsfield and Iaquinta* [2000], who reported based on the balloon borne measurements during the First ISCCP Regional Experiment (FIRE) that the size of ice crystals in cirrus increases from the lower to higher value with rise in temperature. Table 1 and Table 2 summarize the ice nuclei microphysical properties discussed above during the period of observation 2009 and 2010.

Table 5.1: Cirrus clouds ice nuclei properties observed during the period of observation 2009.

Date (dd-mm-yy)	Effective	Radius		Mean Effective Radius (μm)	Cloud Ice Water Content $x10^{-5}$ (g/m^3)	Mean Cloud Ice Water Content $x10^{-5}$ (g/m^3)	Ice Water Path (kg/m^2)	Fall velocity (cm/s)	Ice Nuclei Concentration $x10^3$ (Particles/m^3)	Mean Ice Nuclei Concentration $x10^3$ (Particles/m^3)
	CB	**CM**	**CT**							
21-01-09	15.3	14.4	12.6	14.1	2.98-2.57	5.81	0.15	4.77	7.37-6.36	14.4
28-01-09	16.1	14.7	13.2	14.7	2.96-2.46	7.35	0.18	6.21	6.41-5.33	15.9
11-02-09	15.0	13.2	12.6	13.6	8.59-8.95	12.3	0.31	5.45	23.5-24.5	33.8
04-03-09	20.0	17.6	16.1	17.9	5.01-4.66	12.5	0.38	8.67	6.02-5.6	15.0
01-04-09	15.5	14.4	13.2	14.4	2.65-2.50	3.30	0.08	5.99	6.11-5.77	7.79
29-04-09	21.7	20.3	19.7	20.6	9.19-5.74	15.5	0.31	10.99	7.24-4.53	12.2
13-05-09	19.4	18.8	17.3	18.5	9.33-3.94	15.8	0.40	9.16	10.2-4.29	17.2
03-06-09	23.5	20.6	18.2	20.8	56.8-47.0	87.0	3.48	11.7	43.5-36.0	66.6
22-07-09	*27.3*	*24.1*	*19.4*	*23.6*	*11.4-4.92*	*27.5*	*1.65*	*13.83*	*5.96-2.58*	*14.4*
05-08-09	*29.4*	*25.9*	*19.1*	*24.8*	*18.1-16.7*	*122*	*9.77*	*15.04*	*8.19-7.53*	*55.2*
16-09-09	23.2	18.8	16.7	19.6	5.26-4.55	17.5	0.96	10.1	4.81-4.16	16.0

07-10-09	14.1	13.8	14.1	13.9	2.02-1.72	2.08	0.06	5.65	5.17-4.41	5.34
21-10-09	16.1	15.5	13.5	15.0	2.70-2.39	3.0	0.09	6.43	5.52-4.87	6.14
18-11-09	22.9	20.8	16.7	20.1	6.7-5.3	29.9	1.35	10.54	5.69-4.51	25.4
25-11-09	20.3	18.2	16.4	18.3	4.10-3.44	7.42	0.22	8.99	4.61-3.87	8.40
30-12-09	20.6	18.2	15.8	18.2	4.52-3.65	11.9	0.42	8.91	5.17-4.17	13.6

Table 5.2: Cirrus clouds ice nuclei properties observed during the period of observation 2010.

Date (dd-mm-yy)	Effective Radius (μm)			Mean Effective Radius (μm)	Cloud Ice Water Content x10^{-5} (g/m^3)	Mean Cloud Ice Water Content x10^{-5} (g/m^3)	Ice Water Path (kg/m^2)	Fall velocity (cm/s)	Ice Nuclei Concentration x10^3 (Particles/m^3)	Mean Ice Nuclei Concentration x10^3 (Particles/m^3)
	CB	CM	CT							
06-01-10	18.8	18.2	16.4	17.8	5.51-4.44	5.80	0.03	8.48	6.90-5.65	6.48
13-01-10	19.1	18.2	17.6	18.3	11.3-9.3	14.6	0.09	8.84	11.7-11.3	17.1
03-02-10	24.4	21.1	19.7	21.7	16.9-10.5	35.3	0.42	11.91	10.9-8.06	25.5
10-02-10	18.5	16.7	15.8	17.0	33.6-26.9	58.2	0.44	7.86	46.6-37.2	87.6
17-02-10	18.8	17.6	15.2	17.2	7.98-5.36	12.1	0.11	8.12	10.2-8.44	16.3
17-03-10	22.3	20.3	18.8	20.5	13.5-9.5	20.5	0.18	11.0	9.87-8.37	15.7
28-04-10	23.2	21.7	20.8	21.9	16.0-10.6	45.1	0.34	11.99	9.02-8.86	29.8
12-05-10	23.8	21.7	19.4	21.6	19.5-9.4	86.0	0.90	12.05	14.8-9.84	55.5
11-08-10	18.1	16.7	16.2	17.0	25.3-62.9	158	0.95	8.03	102-29.2	225
01-09-10	15.5	14.4	13.5	14.5	3.08-2.53	3.0	0.02	6.55	6.14-4.97	5.99
22-09-10	15.5	14.4	12.9	14.1	3.21-2.42	3.89	0.03	6.01	6.69-5.77	8.93
13-10-10	*27.0*	*21.1*	*17.9*	*22.0*	*24.1-31.1*	*77.2*	*1.62*	*13.38*	*33.8-7.85*	*53.5*
19-11-10	20.0	16.7	13.5	16.7	92.4-4.24	52.6	0.70	8.14	9.51-71.5	60.3
22-12-10	17.0	15.2	13.2	15.1	5.79-3.61	8.53	0.10	6.92	9.46-7.24	15.3
24-12-10	25.0	23.5	22.0	23.5	365-455	603	4.52	14.25	152-275	308
31-12-10	23.5	20.6	18.2	20.8	15.7-9.0	40.5	0.49	11.88	9.31-7.66	28.7

Dependence of Cirrus Ice Nuclei Microphysical and Optical Properties

The cirrus micro-physical properties such as ice nuclei concentration (INC) and ice water content (IWC) have strong dependence with optical properties such as cirrus extinction, lidar ratio (LR) and linear depolarization ratio (LDR). This helps to understand the formation of clouds and ice nucleation mechanism over the region. Ice nuclei concentration affects the conversion of cloud water to precipitating ice, which is elaborately explained in Bergeron Process[30, 31]. When the ice nuclei concentration is lower than the cloud droplet concentration, efficient conversion of cloud water to ice takes place. When the ice nuclei concentration is greater than or equal to cloud droplet concentration, the growth of ice crystals is limited as there are sufficient super cooled droplets in the cloud.

In order to study the variation of the ice nuclei concentration and ice water content with cirrus extinction, lidar ratio and linear depolarization ratio with altitude, within the cloud, the data corresponding to a typical day is looked into as a case study. The cirrus structure is vertically classified into three: the top layer, middle layer and the bottom layer. The top layer is the upper most one which consists of small ice crystals where the nucleation starts. The middle layer of the cirrus contains pristine ice. The bottom layer is the one in which the ice crystals sublimate due to sub saturation. Figure 14 shows the variation of cirrus extinction, LR, LDR, IWC and INC with altitude observed on 22 July 2009. Table 3 highlights the variation of cirrus extinction, LR, LDR, COD, radius, IWC, IWP, INC and fall velocity with cloud altitude observed on 22 July 2009.
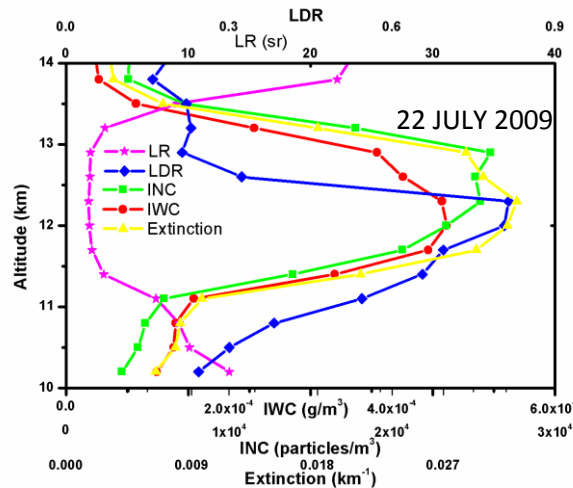

Figure 14: Variation of cirrus extinction, INC, IWC, LR and LDR with altitude observed on 22 July 2009.

Table 3: Altitude variation of micro-physical and optical properties of cirrus cloud observed on 22 July 2009.

Altitude (km)	Extinction (km^{-1})	Radius (μm)	Fall velocity (cm/s)	COD	IWC (g/m^3)	IWP (g/m^3)	INC (particles/m^3)	LDR	LR(sr)
10.2	6.4E-06	28.2	18.6	0.002	1.1E-04	16.7	3.4E+03	0.24	13.4
10.5	7.8E-06	27.4	17.8	0.005	1.3E-04	36.5	4.4E+03	0.30	10.1
10.8	8.2E-06	26.7	17.0	0.007	1.3E-04	56.7	4.9E+03	0.38	9.2
11.1	9.7E-06	26.2	16.5	0.012	1.6E-04	80.3	6.0E+03	0.54	7.4
11.4	2.1E-05	25.4	15.6	0.019	3.3E-04	129.7	1.4E+04	0.66	3.1
11.7	2.9E-05	24.6	14.8	0.029	4.4E-04	196.4	2.1E+04	0.69	2.1
12	3.2E-05	24.0	14.2	0.038	4.7E-04	266.4	2.3E+04	0.81	1.9
12.3	3.2E-05	23.2	13.4	0.047	4.6E-04	335.6	2.5E+04	0.81	1.9
12.6	3.0E-05	22.5	12.7	0.056	4.1E-04	397.7	2.5E+04	0.32	2.0
12.9	2.9E-05	21.6	11.9	0.063	3.8E-04	454.9	2.6E+04	0.21	2.0
13.2	1.8E-05	20.8	11.1	0.067	2.3E-04	489.5	1.8E+04	0.23	3.2

13.5	6.9E-06	20.1	10.6	0.069	8.6E-05	502.4	7.3E+03	0.22	9.1
13.8	3.4E-06	19.3	9.9	0.069	4.0E-05	508.5	3.8E+03	0.16	22.2
14.1	3.1E-06	18.5	9.2	0.070	3.6E-05	513.8	3.9E+03	0.19	23.6

It was observed that the extinction and the lidar depolarisation ratio were maximum at a peak altitude of approximately 12 km. At the same altitude the LR was minimum. The extinction and LDR decreased rapidly above this altitude while LR started increasing. This variation could be well understood by analyzing the cloud layer structure. The upper most layers were having high relative humidity which generates small ice crystals which was less ordered. The size of the ice crystal is low at the cloud top altitude. Hence the ice fall velocity will be too low. The IWC, LDR and extinction were very low at this layer. The middle layer consist pristine ice crystals and it was represented by high depolarisation ratio, optical depth and extinction. At the same time the IWC will also be maximum due to the formation of homogeneous nucleation. The bottom layer had less ice nuclei concentrations due to sublimation and was reflected by low values of depolarisation value, extinction and optical depth. Due to the presence of thick pristine ice crystals at the middle layer, it would have a high optical depth. Also, it can be seen from the table 3 that the COD an IWP were showing an increase with altitude. At the cloud bottom the size of the ice crystal will be maximum and the fall velocity will be high.

Dependence of Cirrus Ice Nuclei Microphysical Properties by Vertical Wind Transport

In order to understand the Indian Summer Monsoon (ISM) activities prevailing over the tropical station we have done a case study for the two days of observations on 22 July 2009 and 05 August 2009, which corresponds to the ISM period. The GPS radiosonde data were used for finding the temperature, pressure, humidity, wind speed and wind direction. Figure 15 and 16 shows the variation of temperature, pressure, humidity, wind speed and wind direction with altitude for the two days of observations on 22 July 2009 and 05 August 2009. It can be seen that the relative humidity was high in the month of August than July 2009 as in general. The cloud altitude ranged from 10.5 to 13.8 km for 22 July 2009 and 9.6 to 14.1 km for 05 August 2009. The cloud geometrical thickness was 3.3 km and 4.5 km respectively. From figure 15 and 16, it can be seen that the for the period 22 July 2009, the vertical wind velocity varied from 12 cm/s to 19 cm/s towards the top of cloud from bottom. Similarly, for 05 August 2009, it varied from 4.5 cm/s to 33.1 cm/s. Hence it was clear that the updraft velocity was not uniform within the same monsoon. There will be slow updrafts as well as fast updrafts. This would also affect the ice formation and its properties. It was clear from the table 1 about the variation of cirrus microphysical properties for the selected days. The IWC, IWP and INC were higher for the cirrus observed on 05 August 2009 compared to 22 July 2009. The cirrus observed on 22 July 2009 was sub-visual (SVC) while on 05 August 2009, dense (DC) in structure. Hence, we can classify the types of cirrus with different formation mechanisms and microphysical properties. The first type of cirrus was the one which formed directly as ice and split in two sub categories, depending on the vertical transport strength: cirrus with slow updrafts were very thin with low IWC and INC; cirrus with fast updrafts were thick with high IWC and INC. The second type of cirrus originates from mixed phase clouds.
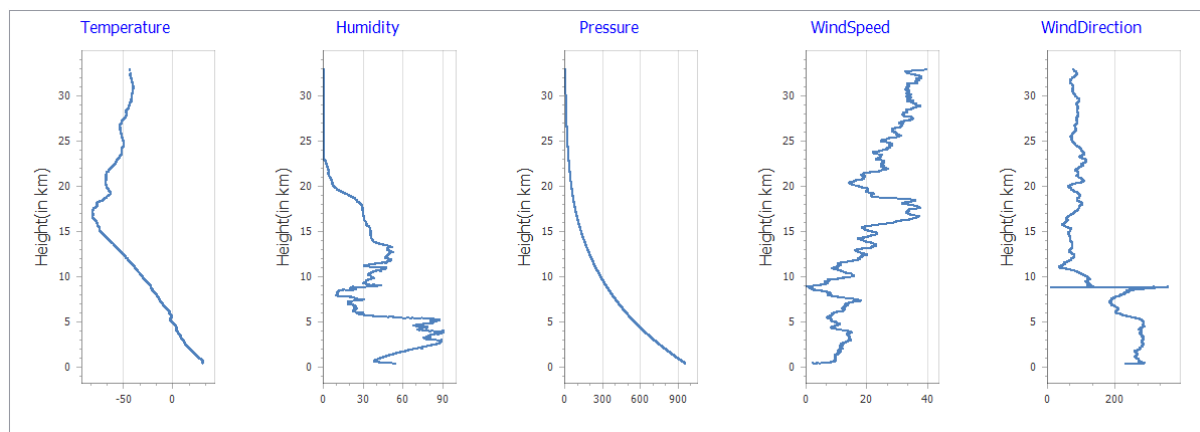

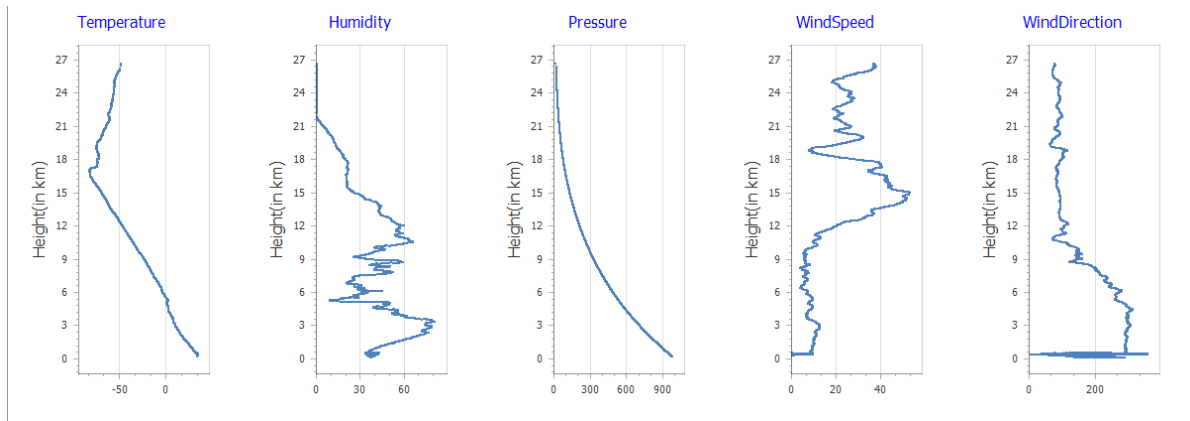**Figure 15:** GPS Radiosonde observations on 22 July 2009.

Figure 16: GPS Radiosonde observations on 05 August 2009.

For thin cirrus (TC) ice nuclei microphysical properties variation, we had taken 13th October 2010 as a case study. The vertical profiling of wind transport from MST Radar analysis of the observed day was shown in figure 17. Figure 17 depicts the effect of zonal (u), meridional (v) and vertical (w) winds components with altitude. The vertical component showed an updraft from the cloud bottom to mid –cloud (12.6 km) with a peak of 60 cm/s and then started downdraft showing reversal in the direction of transport. Also, it was clear that westerly weak zonal wind was active in the cloud bottom and strong easterly wind above the cloud top. The meridional wind component was southerly in nature and act within the cloud region. The observed results were in agreement with the results reported by Rao et al., [2014]. Hence it is clear that the circulation dynamics over the cloud will have a major role in transporting the particulates and water vapor present in the atmosphere.
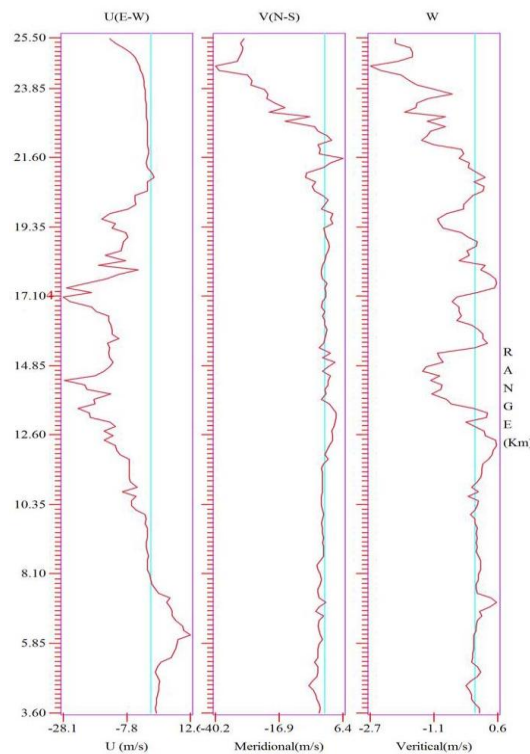

Figure 17: Vertical profile of zonal (u), meridional (v) and vertical (w) winds components with altitude for the observation day 13 October 2010.

IV. Conclusion

Cirrus cloud microphysical parameters were investigated over a tropical station Gadanki, Tirupati during the period of observation from January 2009 to December 2010. The dependence of cirrus optical properties on microphysical characteristics was also discussed. The ice crystal size and its sedimentation (fall) velocity show an increase with decrease in altitude. The ice crystals formed on the cloud top layer were small in

size and less ordered. Above the cloud top altitude, the cirrus extinction coefficient decreases but the size of the ice crystals increases due to heterogeneous formation in the lower stratosphere.

The ice nuclei concentration and ice water content showed strong correlation. The higher ice water content was most frequently observed at the lower altitude where the temperature was warm and the ice crystals formed were aggregates. The cloud middle layer had high depolarisation ratio, optical depth, ice water content, ice nuclei concentration and extinction which suggest the possible mechanism for the formation of cirrus would be homogeneous nucleation. Cirrus formed by slow updrafts were thin with low ice water content and ice nuclei concentration while cirrus with fast updrafts were thick with high ice water content and ice nuclei concentration.

Acknowledgement

References

[1]. Heymsfield, A. J., and G. M. McFarquhar, Mid-latitude and tropical cirrus: Microphysical properties, in Cirrus, edited by D. Lynch et al., Oxford Univ. Press, New York. 2002; pp. 78 – 101.

[2]. Stephens, G.L., Tasy, S.C., Stackhouse, P.W., Flatau, P.J., The relevance of the microphysical and radiative properties of cirrus clouds to climate and climatic feedback, J. Atmos. Sci., 1990; 47, 1742-1753.

[3]. Chen, T., Rossow, W.B., Zhang, Y., Radiative effects of cloud-type variations, J. Clim, 2000; 13, 264-286.

[4]. Intergovernmental Panel on Climate Change (IPCC) Climate Change 2013: The Physical Science Basis. Contribution of Working Group I to the Fifth Assessment Report of the Intergovernmental Panel on Climate Change, Cambridge University Press, Cambridge, United Kingdom and New York, NY, USA, 2013; 1535 pp.

[5]. Fu, Q., An accurate parameterization of the solar radiative properties of cirrus clouds for climate models, J. Climate, 1996; 9, 2058–2082.

[6]. Heymsfield, A. J. and C. M. R. Platt, A parameterization of the particle size spectrum of ice clouds in terms of the ambient temperature and the ice water content, J. Atmos. Sci., 1984; 41, 846– 855.

[7]. Heymsfield, A.J. and G. M. McFarquhar, On the high albedos of anvil cirrus in the tropical Pacific warm pool: Microphysical interpretations from CEPEX and from Kwajalein, Marshall Islands. J. Atmos. Sci., 1996; 53, 2424–2451.

[8]. Heymsfield, A. J. and L. M. Miloshevich, Relative humidity and temperature influences on cirrus formation and evolution: Observations from wave clouds and FIRE II, J. Atmos. Sci., 1995; 52, 4302-4326.

[9]. Dhaman, Reji K. et al., Macro-physical, optical and radiative properties of tropical cirrus clouds and its temperature dependence at Gadanki (13.5° N, 79.2° E) observed by ground based lidar, Ind. J. Rad. and Space Phy., 2016; 45(4), 133-147.

[10]. Rao, P. B., Jain, A. R., Balamuralidhar, P., Damle, S. H., and Viswanathan, G., Indian MST radar 1. System description and sample vector wind measurements in ST mode, Radio Sci., 1995; 30, 1125–1138.

[11]. Hildebrand P. H., and R. S. Sekhon, Objective Determination of the Noise Level in Doppler Spectra, Journal of Applied Meteorology, 1974; 13, 808-811.

[12]. Klett, J.D., Stable Analytical Inversion Solution for Processing Lidar return signals, Appl. Opt., 1981; 20, 211-220.

[13]. Sassen, K, Evidence for liquid-phase cirrus cloud formation from volcanic aerosols: Climatic implications, Science, 1992; 257, 516 – 519.

[14]. Ivanova, D., D. L. Mitchell, W. P. Arnott, and M. Poellot, A GCM parameterization for bimodal size spectra and ice mass removal rates in midlatitude cirrus clouds, Atmos. Res., 2001; 59, 89 – 113.

[15]. McFarquhar, G. M., S. Iacobellis, and R. C. J. Somerville, SCM Simulations of tropical ice clouds using observationally based parameterizations of microphysics, J. Clim., 2003; 16, 1643–1664.

[16]. Platt, C. M. R., and Harshavardhan, Temperature dependence of cirrus extinction: Implications for climate feedback, J. Geophys. Res., 1988; 93, 11,051–11,058.

[17]. Stephens, G. L., Radiative properties of cirrus clouds in the infrared region. J. Atmos. Sci., 1980; 37, 435–446.

[18]. Pruppacher H. R. and J. D. Klett, Microphysics of Clouds and Precipitation, Kluwer Academic Publishers, Dordrecht Netherlands, 1997.

[19]. Heymsfield, A. J., and L. M. Miloshevich, Parameterizations for the Cross- Sectional Area and Extinction of Cirrus and Stratiform Ice Cloud Particles, J. Atmos. Sci., 2003; 60, 936–956.

[20]. Khvorostyanov, V. I., and K. Sassen, Microphysical processes in cirrus and their impact on radiation: A mesoscale modeling perspective, in Collective Monograph ''CIRRUS,'' edited by D. Lynch et al., 2002; chap. 19, pp. 397 – 432, Oxford Univ. Press, New York.

[21]. Mitchell, D. L. et al., Representing the ice fall speed in climate models: Results from Tropical Composition, Cloud and Climate Coupling (TC4) and the Indirect and Semi- Direct Aerosol Campaign (ISDAC), J. Geophys. Res., 2011; 116.

[22]. Liou, K. N., Gu, Y., Yue, Q., and McFarquhar, G, On the correlation between ice water content and ice crystal size and its application to radiative transfer and general circulation models, Geophys. Res. Lett., 2008; 35, L13805.

[23]. Heymsfield, A. J., Extinction-ice water content-effective radius algorithms for CALIPSO, Geophys. Res. Lett., 2005; 32, L10807.

[24]. McFarquhar, G. and A. J. Heymsfield, Microphysical characteristics of three anvils sampled during the central equatorial pacific experiment, J. Atmos. Sci., 1996; 53, 2401–2423.

[25]. Pruppacher H. R. and J. D. Klett, Microphysics of Clouds and Precipitation, Kluwer Academic Publishers, Dordrecht Netherlands, 1997.

[26]. Lawson, R. P. et al., Aircraft measurements of microphysical properties of subvisible cirrus in the tropical tropopause layer. Atmos. Chem. Phys., 2008; 8, 1609–1620.

[27]. Krämer, M. et al., Ice supersaturations and cirrus cloud crystal numbers. Atmos. Chem. Phys. 2009; 9, 3505–3522.

[28]. Kärcher, B., and U. Lohmann, A parameterization of cirrus cloud formation: Homogeneous freezing of supercooled aerosols, J. Geophys. Res., 2002; 107(D2), 4010.

[29]. Heymsfield, A. J., and J. Iaquinta, Cirrus crystal terminal velocities, J. Atmos. Sci., 2000; 57, 916–938.

[30]. Fletcher, N.H., The Physics of Rainclouds, Cambridge University Press, 1969; 309 pp.

[31]. Hobbs, P. V., G. C. Bluhm, and T. Ohtake, Transport of ice nuclei over the North Pacific Ocean, Tellus, Ser. A and Ser. B, 1971a; 23(1), 28–39.